

An Empirical Method for Estimating Thermal System Parameters Based on Operating Data in Smart Grids

Lee Holland, *Student Member, IEEE*, H. Bora Karayaka, *Senior Member, IEEE*, Martin L. Tanaka and Aaron Ball
Department of Engineering and Technology
Western Carolina University
Cullowhee, North Carolina USA
hbkarayaka@wcu.edu

Abstract — An experimental methodology was developed for online system identification of a thermal system or heated space. In this setting, the intelligent controller detects system parameters during normal operation and adapts its performance accordingly. The ultimate goal is to demonstrate that load leveling with demand side management can be used to reduce peak power consumption while maintaining residential room temperatures at a comfortable level. A prototype enclosure was built and equipped with a heater and thermal measuring equipment. Data was collected during a 17 hour temperature regulation experiment using a bang-bang controller similar to those commonly used for residential heating control. First and second order mathematical models were developed for thermal system identification. The mathematical models utilized the collected temperature data to estimate the net thermal resistance and capacitance using system identification techniques. Results showed the second order model to match the real system characteristics reasonably well. It was found that even for a small prototype enclosure, the estimated thermal parameters showed quite large values of thermal capacitance which can be a great asset for demand side management and control applications in a smart grid. The system identification method developed here is an important step toward the development of intelligent controllers.

I. INTRODUCTION

Domestic and commercial buildings use a majority (39%) of the total energy in the U.S. Reducing energy consumption by up to 30% is possible with component upgrades and advanced controls [1]. In 2004, residential buildings accounted for over 20% of the primary energy consumption in the U.S. and a majority of this energy (29%) was used for space heating [2]. A challenge in space heating residential buildings is matching the thermal system to the electric power supplied. Utilizing a system identification strategy with thermostatically controlled appliances (TCA's) may reduce thermal waste without affecting customer comfort.

Demand-side management (DSM) systems have been modeled and implemented for space heaters, electric water heaters (EWH's) and other TCA's. TCA's with loads less than 10kW respond quickly to control signals, but can be undesirable due to rapid changes in room temperature that reduced customer comfort [3]. Direct methods for controlling EWH's for DSM have been shown to save up to 2MW of energy with 33,000 EWH's [4]. A thermal model of a target system may be utilized to ensure customer comfort levels and to calculate power used by the system.

Using an electrical circuit representation of the thermal system can enable the use of system identification techniques to predict system parameters [5]. Once the thermal loads of a system are known, these can be used with a predictive model to save money by accounting for changes in weather and utility prices (Table 1) [1].

In order to determine individual space heater loads, a simple thermal characteristic model is needed to capture each building's unique thermal heating characteristics. The thermal loads can then be used as a passive energy sinks for demand side management and advanced predictive controllers [3]. Such controls can save customers money in the case of dynamic energy pricing and reduce thermal wastes due to inadequate thermal models.

Thermal parameter estimation methods in the published literature utilize various estimation methods for space heating applications [1,7-8]. However, in these models, the electrical power drawn has not specifically been characterized as an input. In this paper, a novel experimental methodology is presented that relates the thermal model to the electrical power supplied. The ultimate goal is to develop an intelligent controller that automatically detects the system thermal parameters using the system identification methods proposed here and uses these parameters for adaptive load regulation.

TABLE 1 – North America Proposed Pricing Structures [6]

Structure	Time of Day	Cost (cents/kWh)	Additional Information
Flat Rate		5.8	First 600kWh of Summer
(FR)		6.7	Additional Use
Time of Use	10pm-7am	3.5	off-peak
(TOU)	7am-11am	7.5	mid-peak
	11am-5pm	10.5	on-peak
Critical Peak Pricing	10pm-7am	3.1	off-peak
	7am-11am		
(CPP)	5pm-10pm	7.5	mid-peak
	11am-5pm	10.5	on-peak
	Event Block	30	CPP 3-4 Hour event Block
Real Time Pricing	Average	5	Price changes relative to
(RTP)	Maximum	35	actual Power generation

The paper is organized as follows: Section II defines the reference thermal circuit models and associated parameter estimation scheme. Section III elaborates on the test setup and data collection methodologies. Section IV presents the results from model parameter estimation and validation procedures. A brief discussion of the results and conclusions are included in Sections V and VI, respectively.

II. SYSTEM IDENTIFICATION SCHEME

A. Thermal Circuit Equivalency

Thermal resistance networks are often used to estimate the rate of heat transfer through a system [9]. In these systems, the heat transfer, temperature, and thermal resistance are analogous to the current, voltage and electrical resistance of an equivalent electrical circuit, respectively. Energy storage in the air and other materials may be represented using capacitors.

Energy balance in a thermal system can be described by

$$\frac{dU}{dt} = P_{in} - \dot{Q}_{out}, \quad (1)$$

where $\frac{dU}{dt}$ is the change in internal thermal energy (kJ/s), P_{in} is the power delivered to the room by the electric heating element (W), and \dot{Q}_{out} is the heat loss through the walls of the building (W). An increase in internal thermal energy results in an increase in temperature according to

$$\frac{dT}{dt} = \frac{1}{m c_p} \left(\frac{dU}{dt} \right) \quad (2)$$

where m is the mass of the thermal system (kg), c_p is the specific heat capacity (kJ/kg·K), and T is the system temperature (K). Total heat transfer is estimated by,

$$\dot{Q}_{out} = \frac{(T_{room} - T_{outside})}{R_{tot}} \quad (3)$$

where, R_{tot} is the total thermal resistance. R_{tot} can account for any combination of convective and conductive heat transfer components. Combining equations 1, 2, and 3 yields

$$P_{in} = \frac{(T_{room} - T_{outside})}{R_{tot}} + m c_p \frac{dT_{room}}{dt}. \quad (4)$$

Two models were developed to represent the thermal dynamics (5) using an electrical circuit analogy. The first is a first order circuit model with a single thermal capacitance (Fig. 1) identical to (5) except for heater thermal resistance R_1 . The circuit dynamics in state space form are

$$\begin{aligned} \dot{x} &= -\frac{1}{R_2 C_1} x + \frac{1}{R_2 C_1} V_1 + \frac{1}{C_1} P_{in} \\ y &= x \end{aligned} \quad (5)$$

where x is the state variable representing room temperature T_{room} and y is the system output T_{room} that is measurable. V_1 is the input representing ambient temperature $T_{ambient}$ or $T_{outside}$. P_{in} is the second input for electrical power supplied. R_1 and R_2 or R_{tot} are the thermal resistances for heaters and enclosure, respectively. C_1 models the combined thermal mass or capacitance which is the same as $m c_p$ in equation 4.

The second is a model with two thermal capacitance levels that also incorporates heater dynamics (Fig. 2). The circuit model in state space form is

$$\begin{aligned} \begin{pmatrix} \dot{x}_1 \\ \dot{x}_2 \end{pmatrix} &= \begin{pmatrix} -\frac{1}{R_2 C_1} & \frac{1}{R_2 C_1} \\ \frac{1}{R_2 C_2} & -\frac{1}{R_2 C_2} - \frac{1}{R_3 C_2} \end{pmatrix} \begin{pmatrix} x_1 \\ x_2 \end{pmatrix} + \begin{pmatrix} 0 \\ \frac{1}{R_3 C_2} \end{pmatrix} V_1 + \begin{pmatrix} \frac{1}{C_1} \\ 0 \end{pmatrix} P_{in} \\ y &= x_2 \end{aligned} \quad (6)$$

where x_1 and x_2 are the state variables that represent heater temperature T_{heater} and room temperature T_{room} , respectively. y

is the system output T_{room} that is measurable. V_1 is the input that represents ambient temperature $T_{ambient}$. P_{in} is the second input for electrical power supplied. R_1 , R_2 and R_3 are the thermal resistances for heater, air and enclosure. The capacitor (C_1) and (C_2) are used to model combined heater and air thermal capacitances in the room.

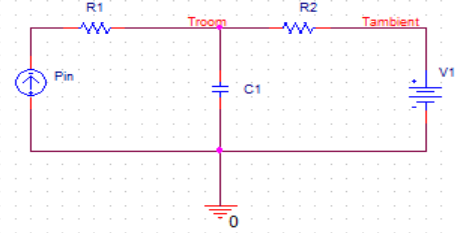


Figure 1 – One Capacitance Thermal Circuit Model

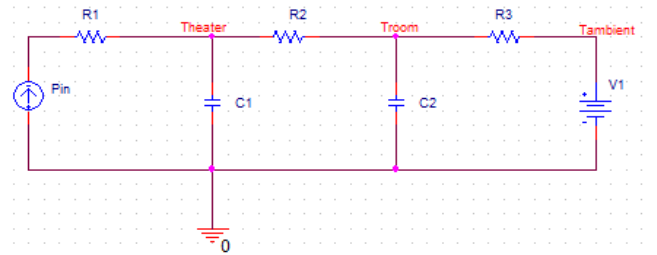


Figure 2– Two Capacitance Thermal Circuit Model

B. Estimation Methodology

The estimation method utilizes a cost function V to minimize error. This cost function can be stated as follows:

$$V(\hat{\theta}) = \frac{1}{N} \sum_{k=0}^N [e^T(k, \hat{\theta}) e(k, \hat{\theta})] \quad (7)$$

where $\hat{\theta}$ is the parameter vector to be estimated, N is the number of samples, and e is the error between estimated and measured output values. e is defined as

$$e(k) = Y(k) - \hat{Y}(k) \quad (8)$$

where $Y(k)$ and $\hat{Y}(k)$ are the system and the model outputs, respectively (Fig. 3). The cost function V can be effectively minimized by using an adaptive version of Gauss-Newton (*gna*) [10] and Levenberg-Marquardt (*lm*) [11] least squares search algorithms.

The parameter estimation vector is $\hat{\theta} = [R_2 \ C_1]$ for the first order model (5) and $\hat{\theta} = [R_2 \ C_1 \ R_3 \ C_2]$ for the second order model (6). The input vector is $U = [P_{in} \ T_{ambient}]$ and the output vector $Y = T_{room}$. Since R_1 is not part of models (5 & 6), it cannot be estimated.

III. TEST SETUP AND DATA COLLECTION

In order to perform system identification, the temperature and power were measured over time to obtain the input-output relationship (Fig. 3). A prototype insulated enclosure with a built in heater was constructed (Fig. 4). The enclosure did not have insulation on the bottom. Using the input power data and the thermal boundary temperatures, system

identification was used to determine the thermal capacitance of each system model and the total thermal resistance of each thermal boundary surface.

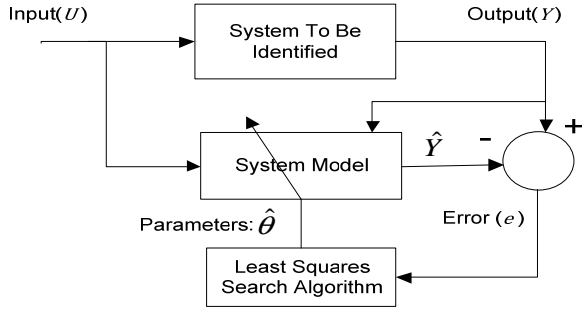


Figure 3 – Parameter Estimation Scheme



Figure 4– Thermal Enclosure with Sensors and Heater Panel

A. Instrumentation

A computer with two instruments was used to collect data from the heated enclosure (Fig. 5). Input power was measured using a Watts UpPro™ meter capable of measuring active power, power factor, and line frequency for 120Vrms appliances with currents up to 15 amps. A NI-cDAQ-9172 with NI 9219 and NI 9205 modules was used to measure voltages of RTD sensors used to determine the temperatures. A built-in Love Controls Series 16A PID controller was used to turn on and off the small resistance heater inside the enclosure.

B. Data Collection

Input power and temperature was monitored using a custom LabVIEW™ program. Power levels were read via the Visa Serial Communication port. A serial command was written for external data logging with a 1 second time interval. Data was then read with a Visa read node whenever a serial command was sent from the power meter. The NI 9219 Module was used with a cDAQ-9172 to read four Honeywell td5a™ three-wire RTD temperature sensors. One sensor was used to measure the room ambient temperature, and three sensors located inside the enclosure at the door, floor, and heater were used to monitor the temperatures of these components (Fig. 4). The RTD's utilized a 5V external source and a voltage divider application circuit that yielded an accuracy of +/- 0.4 degrees Celsius. The voltage across the RTD changed with the temperature and was converted to

temperature in Celsius after the data was collected. Power and temperature data was saved to a text file.

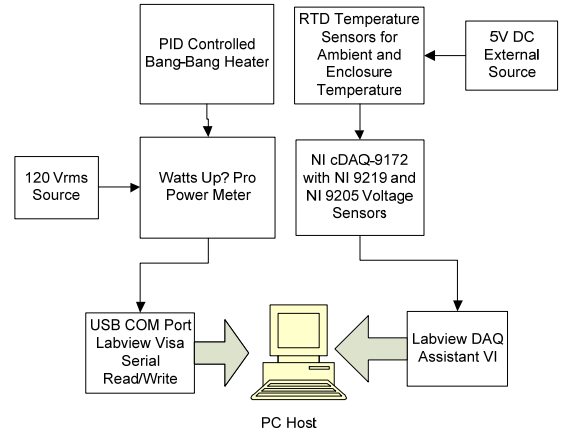


Figure 5 – Data Acquisition Block Diagram

C. Testing Procedure

The testing procedure used a Love Controls Series 16A PID controller that utilized a standard bang-bang controller (turn on/off). The “on” temperature was set at 25.7 °C and the “off” temperature was set at 29.3 °C. The controller used a thermocouple sensor located in the close proximity to the RTD door sensor (Fig. 4). This test was performed with a wooden bottom and generally uniform insulation on the inner walls.

During this test, the data was continuously collected for over 17 hours. The electric power readings were sampled each second and temperature readings were sampled every 1.8 seconds. In order to be consistent for the estimation procedure, the data acquired was reorganized and up-sampled at 2 sec intervals for both temperature and power readings.

IV. RESULTS

The measured data for temperature and electric power readings can be seen in Fig. 6. The first 10,000 seconds of data were removed from the analysis in order to allow the temperature to reach steady state. A total of seven thousand data points (14,000 s) were used in the estimation procedure and the rest of the data are reserved for validation. Throughout the estimation process a function that measures the quality of fit between estimated and measured data was utilized [12]

$$fit(\%) = 100 * \left(1 - \frac{\sqrt{\sum_{k=1}^n (Y(k) - \hat{Y}(k))^2}}{\sqrt{\sum_{k=1}^n (Y(k) - mean(Y))^2}} \right) \quad (9)$$

where Y is measured data and \hat{Y} is estimated model output and the “mean” function denotes the mean value of the array.

The first order thermal model given by (6) was used to estimate R_2 and C_1 . Without a-priori knowledge about the physical parameters, the initial values for R_2 and C_1 were set to 0.15 °C/W and 15,000 W-sec/°C, respectively, to begin the search.

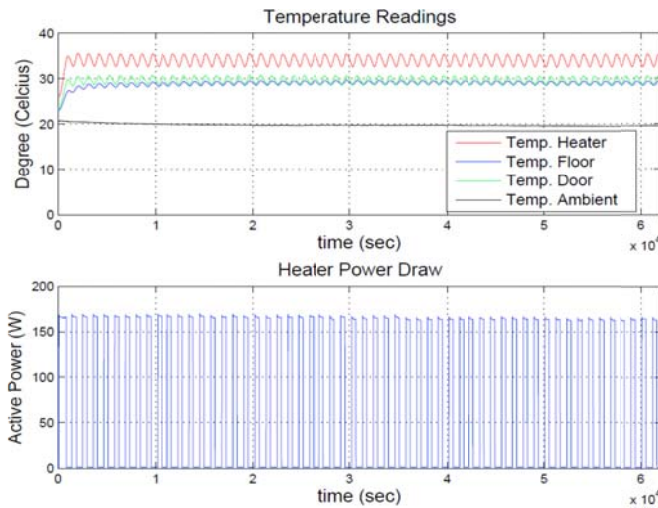


Figure 6- Measurement data acquired for about 62,000 seconds.

The fit between measured enclosure temperature and the first order model is somewhat unacceptable (Fig. 7). The quality of fit was estimated using both *gna* and *lm* search algorithms (Table 2). The system parameters obtained from analysis of samples 5000 through 12000 were validated using data from samples 12000 through 32000. The percent fit obtained for validation was quite close to the fit for the original estimation window. Both of the search algorithms performed identically for R_2 , while there were slight differences in C_1 estimates which had almost no impact on the fit function. Eventually, both search algorithms produced identical fit patterns. One interesting outcome of these estimates was the substantially greater thermal capacitance associated with the floor sensor location which may be explained with the large thermal mass of tile floor.

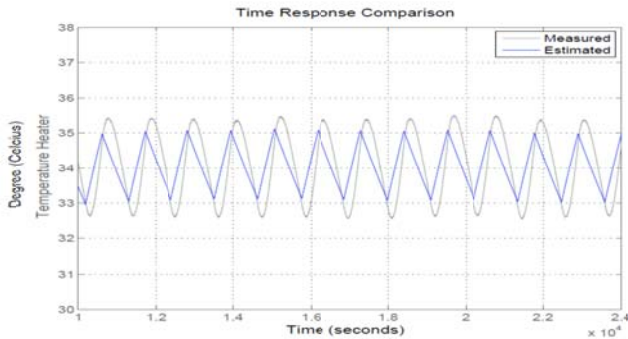


Figure 7 – First order model: Estimated vs. measured data for heater temperature with fit 21.7%

TABLE II. First Order Model Based Thermal Parameter Estimates

Temperature Sensor	R_2 ($^{\circ}\text{C}/\text{W}$)		C_1 ($\text{W}\cdot\text{sec}/^{\circ}\text{C}$)		Fit (%)	
	<i>lm</i>	<i>gna</i>	<i>lm</i>	<i>gna</i>	Estimation	Validation
Heater	0.2221	0.2221	21971	21966	21.7	21.9
Door	0.1544	0.1544	29254	29254	28.4	28.5
Floor	0.1459	0.1459	60299	60295	27.3	22.0

The necessity to investigate a second order model for system identification was evident due to the unsatisfactory fit of the first order model. The estimation window of 7,000 samples was used for the second order model and the four system parameters R_2 , C_1 , R_3 and C_2 were initially estimated.

Initial values for these parameters (without a-priori knowledge) were set to $15\text{ }^{\circ}\text{C}/\text{W}$, $150\text{ W}\cdot\text{sec}/^{\circ}\text{C}$, $0.15\text{ }^{\circ}\text{C}/\text{W}$ and $16\text{ W}\cdot\text{sec}/^{\circ}\text{C}$ respectively. The performance of the second order model was observed to be in good agreement with the measured data (Fig. 8).

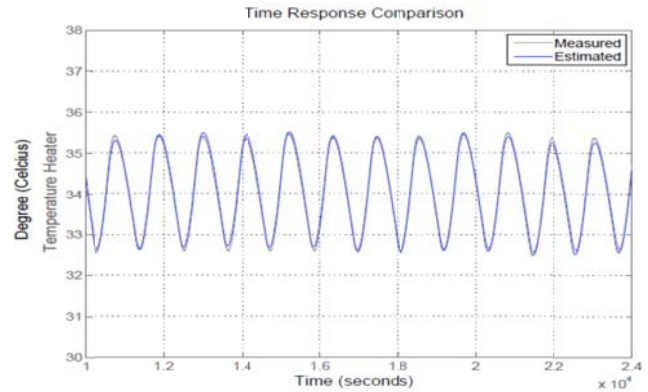


Figure 8 – Second order model: Estimated vs. measured data for heater temperature with fit 90.9%

The validation results also showed good agreement with estimated parameters of the second order model (Fig. 9 & Tables III & IV). The worst fit condition was the estimation of system parameters using the floor temperature data set. However, even in this case, the validation performance was satisfactory (Fig. 10).

TABLE III. Second Order Model Based R_2 and C_1 Estimates

Temperature Sensor	R_2 ($^{\circ}\text{C}/\text{W}$)		C_1 ($\text{W}\cdot\text{sec}/^{\circ}\text{C}$)		Fit (%)	
	<i>lm</i>	<i>gna</i>	<i>lm</i>	<i>gna</i>	Estimation	Validation
Heater	12.578	9.882	130.836	165.715	90.9	92.0
Door	10.759	10.776	189.900	189.672	89.0	90.4
Floor	16.601	9.562	231.414	399.410	82.6	81.1

TABLE IV. Second Order Model Based R_3 and C_2 Estimates

Temperature Sensor	R_3 ($^{\circ}\text{C}/\text{W}$)		C_2 ($\text{W}\cdot\text{sec}/^{\circ}\text{C}$)		Fit (%)	
	<i>lm</i>	<i>gna</i>	<i>lm</i>	<i>gna</i>	Estimation-Validation	
Heater	0.2228	0.2228	1107.5	1113.7	90.9	92.0
Door	0.1551	0.1551	1203.9	1203.8	89.0	90.4
Floor	0.1455	0.1455	1304.9	1313.7	82.6	81.1

The estimated value of R_3 and C_2 values were quite consistent between the two of search algorithm. However, the estimated values for R_2 and C_1 differed based on whether the heater or floor data was used to make the estimations, although the fit percentages were identical for both algorithms. To further investigate this discrepancy, a sensitivity study was conducted to understand the impact of estimated parameter variations on the fit function. In this investigation the estimated parameters for floor temperature data were perturbed by different levels and corresponding fit results were evaluated (Table V).

TABLE V. Estimated Parameter Sensitivities on Fit Function for Floor Data (Original estimation fit of 82.6%)

Perturbation	Fit for R_2 change	Fit for C_1 change	Fit for R_3 change	Fit for C_2 change
+10%	80.4%	80.4%	-80.3%	81.4%
+50%	62.5%	62.4%	-80.3%	68.1%

V. CONCLUSION

An experimental methodology was developed for on-line system identification of a thermal system or heated space. The parameters were estimated and validated using a standard bang-bang controller operating at steady state. Two models were developed and the second order model was found to match the real system characteristics reasonably well.

Even for a small prototype enclosure, the estimated thermal parameters showed quite large values of thermal capacitance which can be a great asset for demand side management and real time control applications in smart grid. The system identification method developed here is an important step toward the development of intelligent controllers.

In future work, demand side management and control methodologies for thermal load leveling based on the estimated parameters will be investigated. In addition, larger varying ambient temperatures will be considered to model outdoor conditions.

ACKNOWLEDGMENT

The authors wish to thank the Center for Rapid Product Realization at Western Carolina University, Prof. Gardner and Prof. Zhang for the project support, and Prof. Adams and Prof. Yanik for helpful suggestions.

REFERENCES

- [1] P. Radecki and B. Hency, "Online building thermal parameter estimation via unscented kalman filtering," in American Control Conference (ACC), 2012, 2012, pp. 3056-3062.
- [2] P. Waide, J. Amann and A. Hinge, "Energy efficiency in the north american existing building stock," OECD/IEA, France, 2007.
- [3] D. S. Callaway, "Can smaller loads be profitably engaged in power system services?" in *Power and Energy Society General Meeting, 2011 IEEE*, 2011, pp. 1-3.
- [4] J. Kondoh, Ning Lu and D. J. Hammerstrom, "An Evaluation of the Water Heater Load Potential for Providing Regulation Service," *Power Systems, IEEE Transactions on*, vol. 26, pp. 1309-1316, 2011.
- [5] G. L. Skibinski and W. A. Sethares, "Thermal parameter estimation using recursive identification," *Power Electronics, IEEE Transactions on*, vol. 6, pp. 228-239, 1991.
- [6] M. H. Nehrir, Runmin Jia, D. A. Pierre and D. J. Hammerstrom, "Power management of aggregate electric water heater loads by voltage control," in *Power Engineering Society General Meeting, 2007. IEEE*, 2007, pp. 1-6.
- [7] Ion Hazyuk, Christian Ghiaus, David Penhouet, "Optimal temperature control of intermittently heated buildings using Model Predictive Control Part I Building modeling," *Building and Environment* 51 (2012) pp 379-387, Elsevier.
- [8] Aaron Smith, Rogelio Luck, Pedro J. Mago, "Integrated parameter estimation of multi-component thermal systems with demonstration on a combined heat and power system," *ISA Transactions* 51 (2012) 507–513, Elsevier.
- [9] Y. Cengel, *Introduction to Thermodynamics and Heat Transfer*. McGraw-Hill Science/Engineering/Math, 2007.
- [10] Wills, Adrian , B. Ninness, and S. Gibson. "On Gradient-Based Search for Multivariable System Estimates" *IFAC World Congress*, Prague, 2005.
- [11] K. Levenberg, "A Method for the Solution of Certain Problems in Least Squares," *IEEE Transactions on Circuits and Systems*, vol. CAS-26, 1979.
- [12] Matlab 2012a System Identification Toolbox.

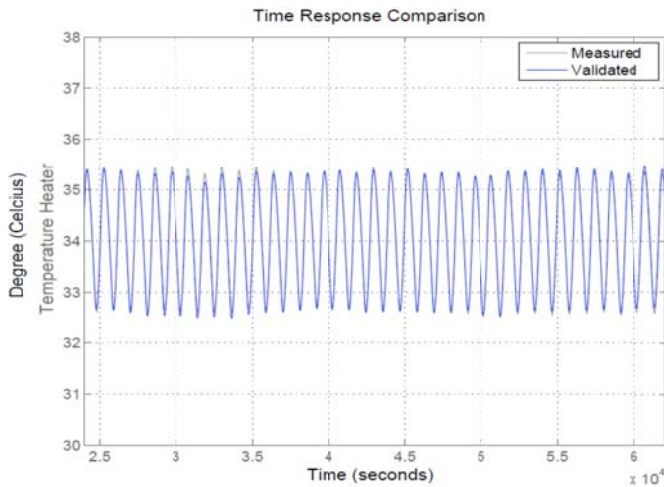


Figure 9 – Second order model: Measured vs. validated data for heater temperature with fit 92.0%

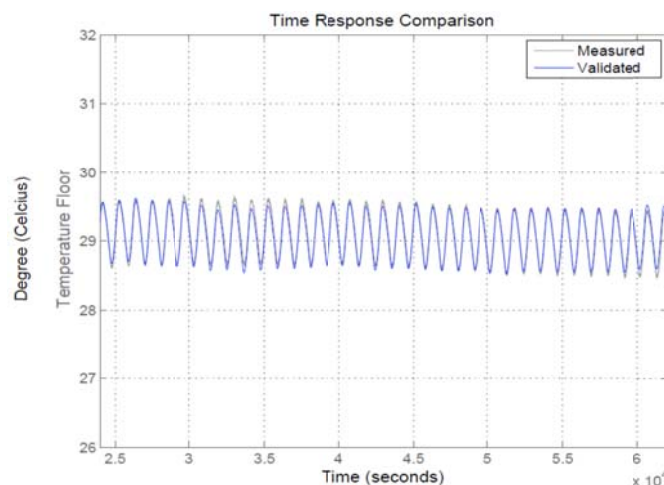


Figure 10 – Second order model: Measured vs. validated data for floor temperature with fit 81.1%

R_3 showed the highest sensitivity and therefore the highest confidence in estimation. C_2 had the least sensitivity and confidence. The sensitivities of R_2 and C_1 were almost identical which leads to a form of dependence between R_2 and C_1 in estimation. In fact, it can be realized by a closer look into Table III that the product of R_2 and C_1 will yield quite similar values for both search algorithms (Table VI).

TABLE VI. Second Order Model Based R_2C_1 Time Constant Estimates

Temperature Sensor	R_2C_1 (sec)	
	<i>lm</i>	<i>gna</i>
Heater	1645.6	1637.5
Door	2043.2	2043.9
Floor	3841.7	3818.9

In addition to the sensitivity study, the uncertainties for the estimated second order model were investigated using the Matlab™ System Identification Toolbox. The uncertainties in C_2 , R_3 and R_1C_2 (combined) for both algorithms were approximately $\pm 10\%$. However, separate C_1 and R_2 estimation uncertainties were reasonably larger which also pointed to the discrepancies in their estimates. In this case, *gna* algorithm yielded smaller uncertainties in comparison to *lm* algorithm.